Pilot production and advanced development of large-area picosecond photodetectors

Michael J. Minot*[a] (mjm@incomusa.com), Bernhard W. Adams [a], Melvin Aviles [a], Justin L. Bond [a], Christopher A. Craven [a], Till Cremer [a], Michael R. Foley [a], Alexey Lyashenko [a], Mark A. Popecki [a], Michael E. Stochaj [a], William A. Worstell [a], Anil U. Mane[b],Jeffrey W. Elam[b], Oswald H. W. Siegmund[c], Camden Ertley[c], Henry Frisch[d], Andrey Elagin[d],
[a] Incom, Inc, Charlton, MA, USA; [b]Argonne National Laboratory, Lemont, IL, USA;
[c]University of California, Berkeley, CA USA; [d]University of Chicago, Chicago IL, USA

ABSTRACT

We report pilot production and advanced development performance results achieved for Large Area Picosecond Photodetectors (LAPPD™). The LAPPD™ is a microchannel plate (MCP) based photodetector, capable of imaging with single-photon sensitivity at high spatial and temporal resolutions in a hermetic package with an active area of 400 square centimeters[1]. In December 2015, Incom Inc. completed installation of equipment and facilities for demonstration of early stage pilot production of LAPPD™. Initial fabrication trials commenced in January 2016. The "baseline" LAPPD™ employs an all-glass hermetic package with top and bottom plates and sidewalls made of borosilicate float glass. Signals are generated by a bi-alkali Na_2KSb photocathode and amplified with a stacked chevron pair of "next generation" MCPs produced by applying resistive and emissive atomic layer deposition coatings to borosilicate glass capillary array (GCA) substrates[2,3,4,5] Signals are collected on RF strip-line anodes applied to the bottom plates which exit the detector via pin-free hermetic seals under the side walls[6]. Prior tests show that LAPPD™s have electron gains greater than 10^7, sub-millimeter space resolution for large pulses and several mm for single photons, time resolutions of 50 picoseconds for single photons, predicted resolution of less than 5 picoseconds for large pulses, high stability versus charge extraction, and good uniformity[7]. LAPPD™ performance results for product produced during the first half of 2016 will be reviewed. Recent advances in the development of LAPPD™ will also be reviewed, as the baseline design is adapted to meet the requirements for a wide range of emerging application. These include a novel ceramic package design, ALD coated MCPs optimized to have a low temperature coefficient of resistance (TCR) and further advances to adapt the LAPPD™ for cryogenic applications using Liquid Argon (LAr). These developments will meet the needs for DOE-supported R&D for the Deep Underground Neutrino Experiment (DUNE), nuclear physics applications such as EIC, medical, homeland security and astronomical applications for direct and indirect photon detection.

Key Words: microchannel plate, MCP, large area photodetectors, LAPPD, picosecond timing, photocathode, pilot production

INTRODUCTION

The LAPPD™ was developed by the Large Area Picosecond Photodetector Collaboration, which in 2009, brought together university, national laboratory and commercial researchers with the goal of developing an MCP based photodetector, capable of imaging, with high single-photon sensitivity, high spatial and temporal resolution, in a hermetic package with a minimum 400 cm^2 active area. Figure 1 shows (top) an exploded view of the LAPPD™ as originally designed by the Collaboration. A top view of the LAPPD™ V1.0, as currently produced by Incom, with X-spacers, and top MCP visible through the top window and photocathode is shown at bottom left;. The internal anode strip-lines are visible (bottom right), through the transparent glass bottom LAPPD™.

Hard X-Ray, Gamma-Ray, and Neutron Detector Physics XVIII, edited by Ralph B. James, Michael Fiederle, Arnold Burger, Larry Franks, Stephen A. Payne, Proc. of SPIE Vol. 9968, 99680X · © 2016 SPIE · CCC code: 0277-786X/16/$18 · doi: 10.1117/12.2237331

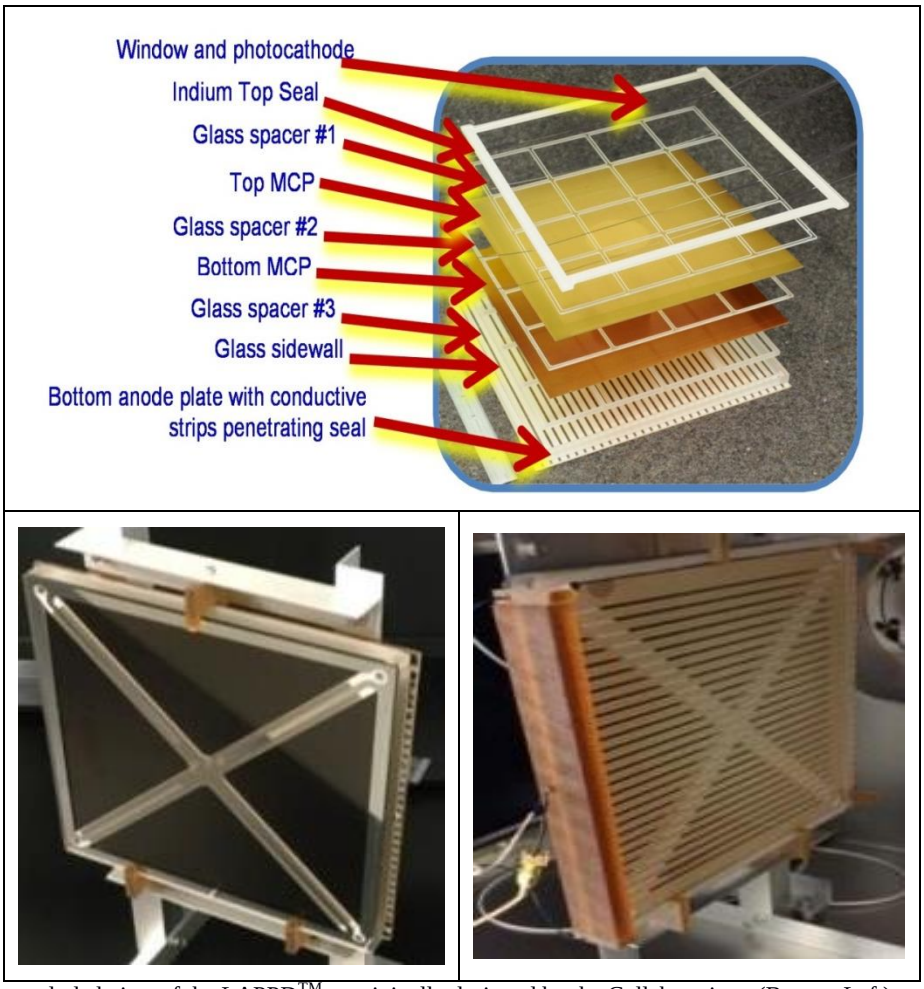

Figure 1 – (Top) an exploded view of the LAPPD™ as originally designed by the Collaboration. (Bottom Left) a top view of the LAPPD™ V1.0, as currently produced by Incom, with X-spacers, and top MCP visible through the top window and photocathode. (Bottom Right), a view of the LAPPD™ transparent glass bottom, showing the internal anode strip lines.

MCP detectors, despite their high speed, were not considered for applications that require large-area coverage due to the small size, high-cost / area, and poor lifetime [8] of those that were commercially available. It is now acknowledged that large area, affordable, very fast photodetectors with micron space resolution and time resolutions below 10 picoseconds (psec) would be a disruptive technology across all three (energy, intensity, and cosmic) of the physics frontiers supporting experiments addressing questions such as the origin of mass, neutrino physics and proton decay, and the nature of dark matter and energy [9]. In addition to high energy physics (HEP), this development will benefit many other areas including: homeland security, astronomy, space instrumentation, remote night time sensing, TOF mass spectrometry, plenoptic and medical imaging (PET scanning) and others.

"Demountable" - The "demountable" was an experimental test stand that allowed standard LAPPD components to be assembled with an O-ring seal between the top window and the body of the photodetector, and tested while the tile was being dynamically pumped. Since a bialkali photocathode cannot tolerate ambient exposure, an aluminum photocathode was used. While a thin metal film of aluminum can serve as a photocathode, it typically has a low quantum efficiency (QE), however when used with a laser source, the light intensity is sufficient to allow reliable testing. The "demountable" allowed performance to be determined, well ahead of the ability to produce fully integrated, free standing sealed detectors with bialkali photodetectors. Performance results [6] were as follows: absolute time resolutions for single-photoelectrons were consistently < 100 psec, and typically < 60 psec; for large pulses projected time resolutions were < 5 psec. Spatial resolution determined for single photoelectrons was several millimeters, while for large pulses a spatial resolution of 700-750 microns was demonstrated. The "demountable" is shown in Figure 2 (top left) including electrical taps that contact the anode strip-lines that pass under the sidewalls of the detector through a hermetic seal. The

location of a signal along the strip-line is determined by precisely measuring the differential time delay of signals moving in each direction as shown in Figure 2 right. Figure 2 bottom left shows the measured 50 psec Transit Time Variation for Single Photoelectron.

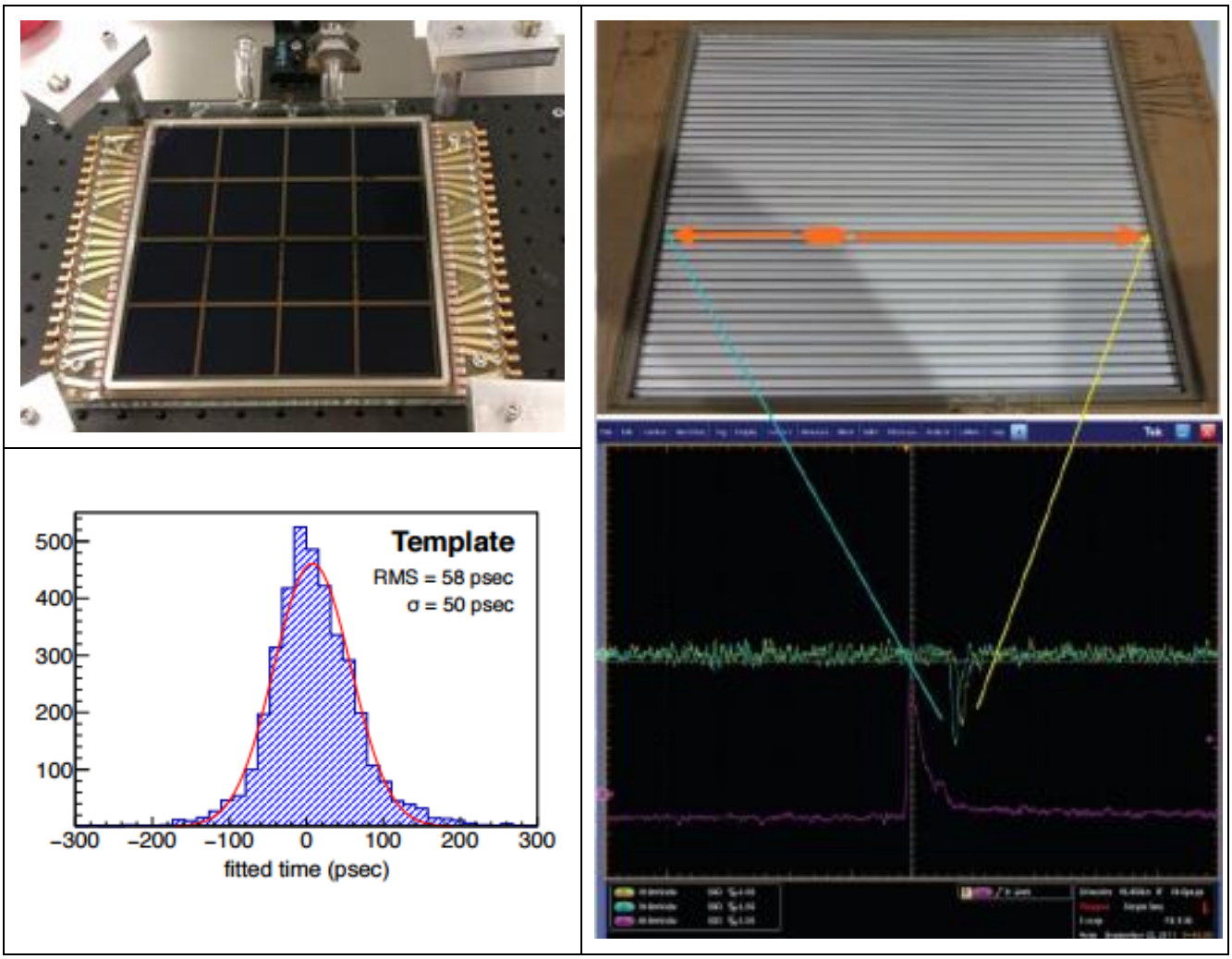

Figure 2 – The "demountable" is shown top left. The location of a signal along the strip-line is determined by precisely measuring the differential time delay of signals moving in each direction as shown on the right. The measured 50 psec Transit Time Variation for Single Photoelectron is shown bottom, left.

These results made it apparent that the next challenge was to establish a pilot production facility, establish routine fabrication of the large area microchannel plates that were the enabling technology for the LAPPD^{TM}, and to replicate the performance results demonstrated with the demountable, with a fully sealed photodetector incorporating a bialkali photodector. In April 2014, the Department of Energy awarded Incom Inc. a two year contract to establish that facility and to demonstrate a pathway toward pilot production [10].

LAPPD^{TM} V1.0 Design - The design of the LAPPD^{TM} currently being fabricated at Incom Inc. was modified to allow independent application of voltage to the top and bottom of each of the two ALD-GCA-MCPs. Key design features are shown in Figure 3.

a) Top left – Lower Tile Assembly (LTA) including borofloat glass bottom with conductive strip-line anodes applied to the inside surface, indium alloy filled grooved sidewalls, hermetically sealed to the bottom plate, allowing strip-line anodes to pass in and out of the evacuated tile without any penetrating pins.

b) Top right – side view of the LTA, showing sidewalls hermetically sealed to the bottom anode plate.

c) Bottom left – showing a chevron pair of ALD-GCA-MCPs separated with X-spacers, sitting in a pre-fabricated lower tile assembly (LTA) the bottom of which is the detector anode. X-spacers restrain window deflection under atmospheric pressure, control and provide critical spacing between components, and support for getters. A borofloat or optional fused silica glass window sits on top and is hermetically sealed to the sidewalls with a low melting indium alloy.

d) Bottom middle - Lower Tile Assembly (LTA), consisting of borofloat glass sidewalls and bottom anode plate, hermetically sealed together. Thin film power & signal anode strips pass under the hermetic seal providing a "penetration free" connection into and out of the tile. Internal corner pins hold components and deliver voltage to the top and bottom of each MCP.

e) Bottom right – a side view showing the stack-up of components, and the groove in the sidewall that retains the molten indium alloy used for top window sealing.

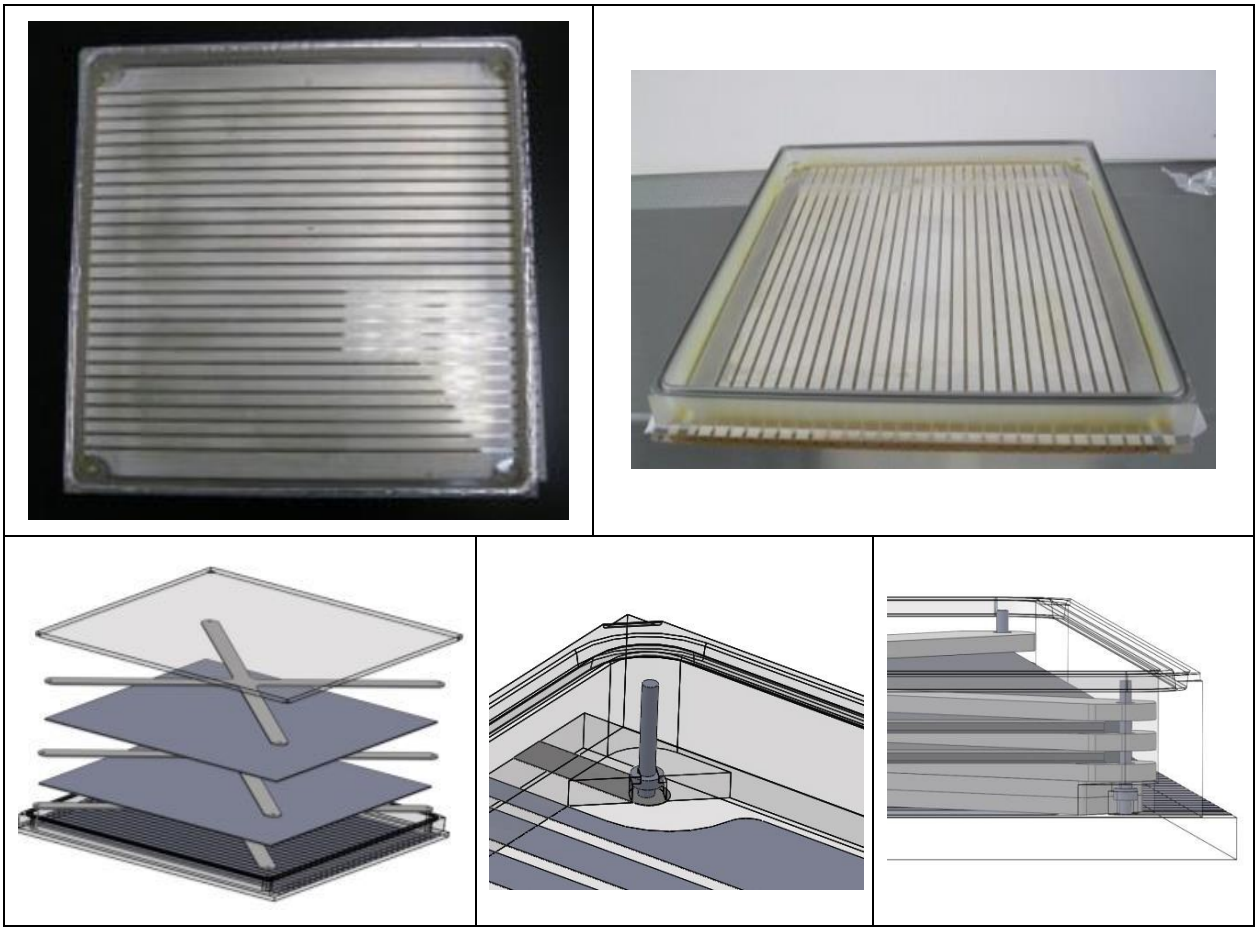

Figure 3 – Showing the construction of the LAPPD^{TM} V1.0

ALD-GCA-MPC Manufacture - One of the enabling technologies for the LAPPD^{TM} is the large area microchannel plate which provides signal amplification. This MCP, the world's largest, is made by a novel technique that uses atomic layer deposition (ALD) to apply resistive and emissive layers to a GCA to produce the "ALD-GCA-MCP". The ALD-GCA-MCP is so named to differentiate it from conventional lead oxide MCPs, and conventional lead oxide MCPs that have been enhanced with an ALD applied secondary emissive layer. Figure 4 depicts the process for fabricating large blocks of glass capillary array material using Incom's hollow core technique. These blocks, approximately 229 mm X 229 mm X 406 mm can produce ~140-150 203mm square glass capillary array (GCA) wafers that serve as substrates for application of resistive and emissive coatings applied by ALD, as depicted in the sketch [11], lower left. Once coated, the microchannel plate (MCP) amplifies signals as shown in the sketch [12], lower right.

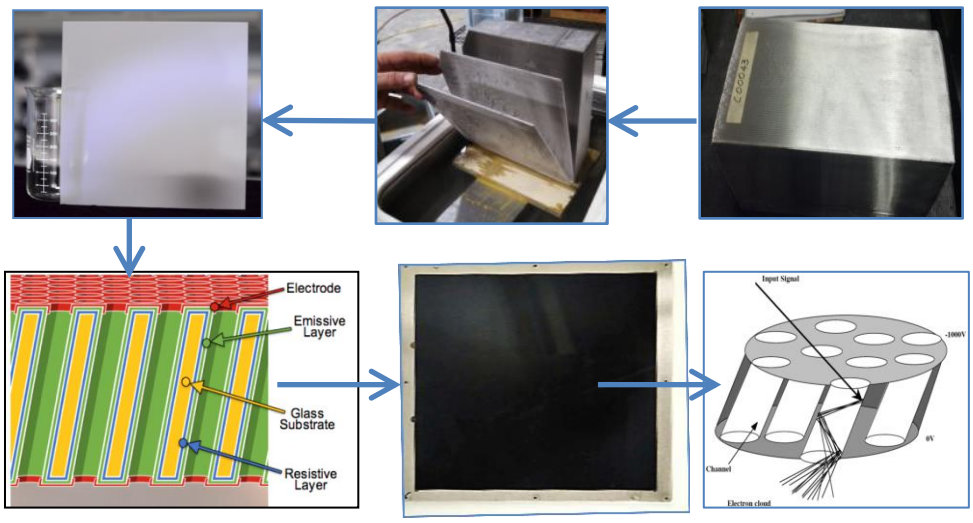

Figure 4 right to left: Incom uses a "Hollow Core Process" to produce large blocks of capillary array material that can be sliced, producing GCAs. Bottom, left to right: Resistive and emissive coatings are applied to these GCA wafers by atomic layer deposition to convert the GCA to an ALD-GCA-MCP. Signal amplification is achieved as shown in the sketch, lower right

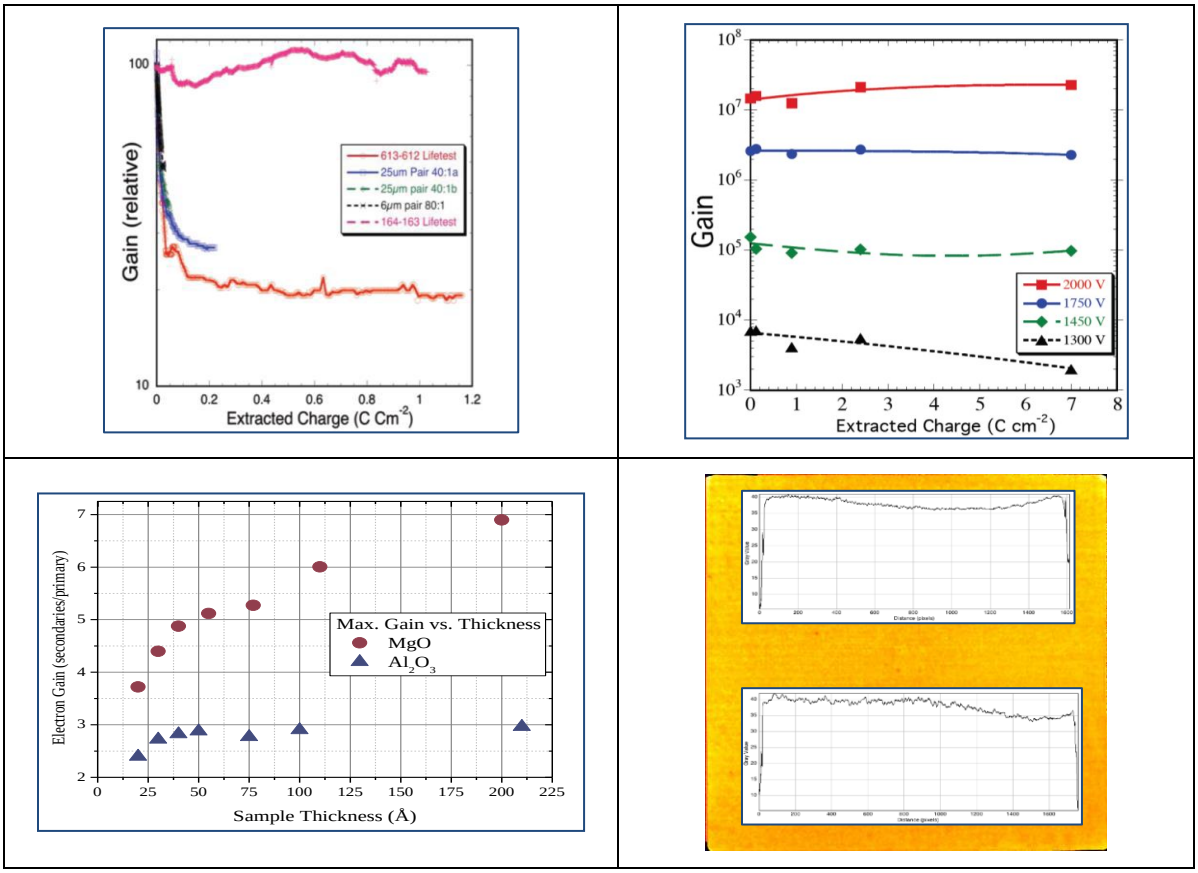

Figure 5 Performance achieved with ALD-GCA-MCPs

The performance achieved with ALD-GCA-MCPs is shown in Figure 5, top left; Conventional MCPs require an extensive "burn-in" and the gain often drops significantly (factor of 5) after burn in before stabilizing. Little burn-in is required for ALD-GCA-MCPs indicated by the violet colored line in the plot [13]. Top right chart shows MCP gain vs.

voltage, showing that the gain for a pair of 33 mm, 60:1 L/D, 20 µm pore ALD-GCA-MCPs remains high and stable even after extracting 7 C/cm^2 charge at ~3 µA [14]. The plot shown in Figure 5 bottom left shows the secondary electron yield as a function of thickness, of the secondary electron emissive layer, which is typically either MgO or Al_2O_3, both of which have high secondary emissive yield [15]. As shown in Figure 5 bottom right, gain uniformity across full area of ALD-coated 203 mm square MCP is typically within ~15%. The gain map image shown is for a pair of 20 µm pore, 60:1 L/D, ALD borosilicate MCPs, measured at 950 volts per MCP, with 184 nm UV exposure. Table 1 provides a summary of ALD-GCA-MCP attributes and competitive advantages.

Table 1 - Summarizes ALD-GCA-MCP attributes and competitive advantage

MCP Attribute	ALD-GCA-MCP Competitive Advantage
Tunable	Independent selection of glass substrate and tuning of resistive and emissive properties.
Gain Stability, Burn-in	High (10^5-10^7) overall gain, long-term temporal stability, minimal burn-in Vs. conventional MCPs that experience 5-10X gain drop and require extended (200 hrs) charge extraction. Hydrogen free process, negligible ion feedback.
Low Dark Count (cm^{-2} s^{-1})	10-25 X Lower dark count (0.025-0.040 vs. 0.25-1.0) since for ALD-GCA-MCPs contain little or no radioactive isotopes, **Enhanced S/N.**
High SEY	~2.5 – 3.5 for conventional vs. ~2.5 to 3.0 and ~4 to 7 for Al_2O_3 and MgO SEE Layers. **Higher Gain Sensitivity**
Low X-ray Cross-Section	No lead, for **application in an X-ray background**.
TCR (K^{-1})	Semiconductor like behavior with TCR = ~-0.01 to -0.03 for conventional, and ~ -0.02 to -0.04 for ALD-GCA-MCPs
Pore Size & OAR	10 µm pores, with OARs up to 74% in large plate sizes for enhanced detection efficiency; and spatial and temporal resolution.
Large Size	203mm X 203mm MCPs wafers, **the world's largest**
Gain uniformity	Within 15% across 203mm x 203mm plates with 20 µm pores
Robust MCPs	No H_2 firing or acid etching, that make conventional lead silicate MCPs fragile, moisture sensitive and prone to shape distortions. **Chemically, thermally and mechanically stable**.
Curved Shape	Enhanced resolution for space and terrestrial TOF instrumentation, simplified design, reduced instrument volume, cost and mass.
Lower cost per area	Large area MCPs, diced to smaller sizes, low cost glass substrates with independently optimized resistive and emissive coatings results in enhanced performance with significant cost and design flexibility.

Detector Tile Integration & Sealing - Final assembly of the LAPPD, including deposition of the photocathode, and final sealing, is done in an ultra-high vacuum (UHV) tank depicted in *Figure 6*, equipped with conflat seals, scroll, turbo and ion pumps. Tile kit components are pre-assembled & loaded in place, and then baked @ 350C to a low 10^{-10} torr range.

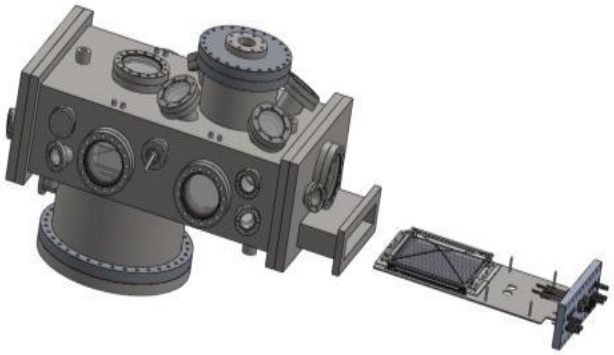

Figure 6 - Final assembly of the LAPPD^{TM} is done in an ultra-high vacuum (UHV) tank.

After in-tank scrubbing of the ALD-GCA-MCPs, the Na_2KSb photocathode is applied at an elevated temperature using SAES alkali-metal dispensers. Development of the photocathode can be monitored by measuring photocurrent. The

absolute quantum efficiency of photocathode can be measured using NIST calibrated photodiodes. Once the photocathode is deposited, the window is moved back using an in-vacuum window transfer process and lowered onto the detector sidewalls where it forms a hermetic seal as the molten indium alloy cools. The current set-up provides for limited measurement of the detector performance while it is still in the tank.

Pilot production commissioning trials - Pilot production commissioning trials were begun in January 2016, following a two year construction period in which pilot production infrastructure including equipment and clean room facilities were completed. The goal of these trials was to identify and resolve technical issues ultimately leading to a routine process for fabrication of fully integrated, free standing LAPPD*TM*. Multiple leak tight indium top window seals were made demonstrating that sealing along the 812mm perimeter of the LAPPD™ was not a barrier to success, while also achieving a major interim program goal. Process variables affecting the ability to produce effective, high QE photocathodes were understood and optimized achieving QEs that varied from 1% to 12% @ 365 nm and 190C. A "manufacturing pipeline" for tile kit components, including large area ALD-GCA-MCPs was created at Incom to insure that the pace of future manufacturing would not be limited by supply of these critical path components. In addition, LAPPD™ tiles were assembled, sealed and tested, demonstrating a pace of 2 tiles / month with the current UHV integration & sealing unit, with ample opportunity for cycle time reduction and scale-up to higher volumes. Detector tile design was optimized to eliminate stack-height variability issues which were a major cause of failure for a number of the early tile trials. Another area of concern was whether specially prepared sealing surface along the edge of the top window were being contaminated with alkali metals during photocathode deposition, preventing a good seal.

The Important Role of "Stack Height" – The LAPPD™ incorporates X-spacers that define the spacing between the photocathode and the top of the entry MCP, between the bottom of the entry MCP and the top of the exit MCP, and the bottom of the exit MCP and the top of the anode. In addition to maintaining these critical dimensions, the X-spacers provide internal support that opposes the force of atmospheric pressure, and prevents stress fracture of either the glass top window or bottom anode plate. Finite element analysis shows that these stresses are greatest along the perimeter of the sidewalls and in the open areas between the "Xs" and that the stresses that develop depend on the amount of deflection of these glass plates. Stack height (SH) is defined as the distance between internal tile components and the sidewall sealing surface when compressed under atmospheric pressure. If stack height is low, window deflection can be excessive leading to stress fracture of either the top window or bottom anode. If stack height is too high, the top window might not contact the liquid indium alloy bead uniformly, resulting in a failed seal. After multiple failures due to too high or too low of a stack height, the internal design and material selection for X-spacers was simplified to minimize SH variability, greatly improving the probability of success.

Fused Silica Windows – For many LAPPD™ applications, the enhanced UV transmission of fused silica is required. Fused silica was used as the top window for tiles #7, #8 and #9 demonstrating that it can be sealed with indium alloy to the borofloat sidewalls despite a significant difference in the coefficient of thermal expansion. In addition to enhanced UV transmission, fused silica offers the additional advantage of higher strength compared to an equivalent thickness of borofloat glass.

Top Window Preparation for Photocathode deposition & Indium Sealing - Photocathode is deposited on the inside surface of the top window. Light transmitted through the window impinge on the photocathode, convert to electrons that are accelerated toward the top MCP under the voltage potential between it and the photocathode. Preparation of the window, prior to photocathode deposition, includes application of thin film electrodes that allow electrical contact and charge replenishment to the photocathode, and includes proprietary cleaning procedures that affect the quality and responsiveness of the photocathode. Additional thin metal film coupling coatings are applied to the inside perimeter of the top window to insure a strong bond between the indium alloy and the glass window. Contamination of the indium sealing surface with alkali during photocathode deposition is believed to compromise the quality of the seal surface preparation, contributing to leaks.

Figure 7 (top) shows the photocathode QE for LAPPD™ #7. QE measurements are done during deposition, while the PC is still hot. Prior experience shows that the bi-alkali photocathode QE will increase upon cooling, as shown (bottom left) for PC Shoot #6 which increases as the film cools (red, as-deposited at 190C on 4/7/2016, and at room temperature on 4/8 dark blue, on 4/11 light blue, and on 4/20 black). QE *deposition* had been previously shown to be uniform over a *400 c*m square area as shown in the lower right figure [16].

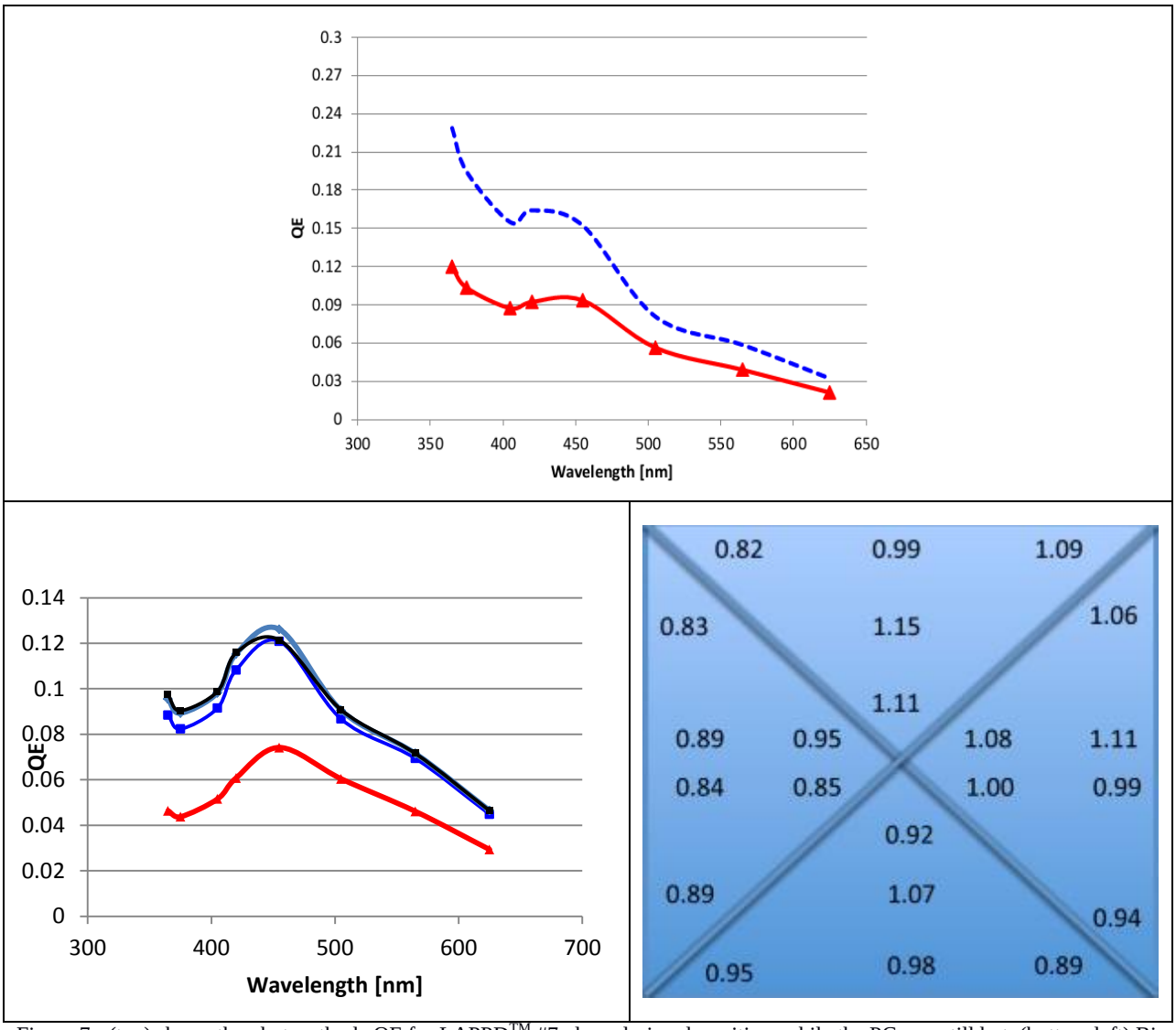

Figure 7 - (top) shows the photocathode QE for LAPPD™ #7, done during deposition, while the PC was still hot, (bottom left) Bi-alkali photocathode QE increases upon cooling: red, as-deposited at 190C on 4/7/2016, and at room temperature on 4/8 dark blue, on 4/11 light blue, and on 4/20 black, (bottom right) QE uniformity had been previously shown to be uniform over a 400 cm square area.

Tile trial #9 was designed to use a thin film aluminum metal photocathode, as the first of a series of trials to evaluate whether alkali spill-over onto the critical indium sealing surfaces was contributing to earlier sealing problems. Figure 8 shows the gain vs. voltage for the MCP pair used. The voltages applied to the stack was -2,600 to the photocathode, -2,400 and -1,400 respectively to the top and bottom of the entry ALD-GCA-MCP, -1,200 and -200 respectively to the exit ALD-GCA-MCP. The corresponding gain, for those voltages, is 3 X 10^6 based upon the earlier measurements as shown in Figure 8.

LAPPD™ #9 was completed and removed from the UHV tank on September 14th, 2016. The limited testing done to date convincingly demonstrated that the tile sealed properly and was functional, at a level consistent with our expectations for an aluminum photocathode [17]. Figure 9 shows pulses recorded under ambient full atmosphere conditions, when exposed to a Hg(Ar) lamp. The pulse rate doubles when the lamp is turned on. The threshold trigger rate for the oscilloscope was set high due to periodic noise from the lamp. Further ambient testing of the tile was performed employing various illumination scenarios as shown in Figure 10.

Figure 10 shows the anode current over time, as the Hg(Ar) lamp was turned on, then the photocathode turned off, then the Hg(Ar) lamp turned off, and finally with a 360nm LED turned on. The photocathode was "turned off" by reversing

the electric field in the gap between the entry window and the top face of the entry ALD-GCA-MCP thus blocking photoelectrons from entering the ALD-GCA-MCP. In this "photocathode off" mode anode current was still detected, because the UV light was able to stimulate emission of electrons from the top of the entry ALD-GCA-MCP, which were amplified by the ALD-GCA-MCPs and extracted from the anode. With the lamp turned off the dark current, read at the anode strips, was about 13nA.

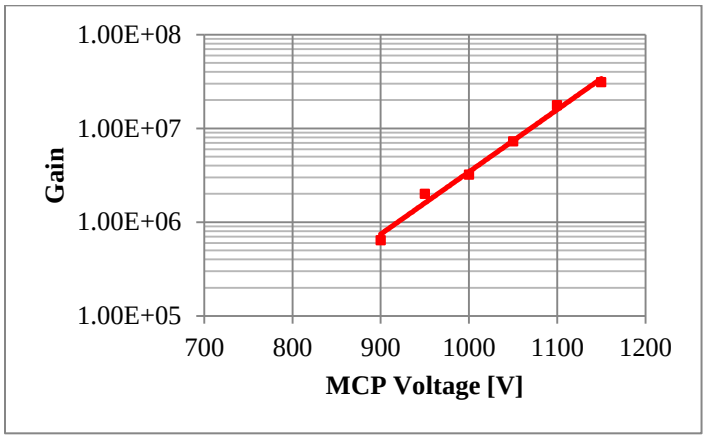

Figure 8 – Gain vs. voltage for the MCP pair used in LAPPD #9

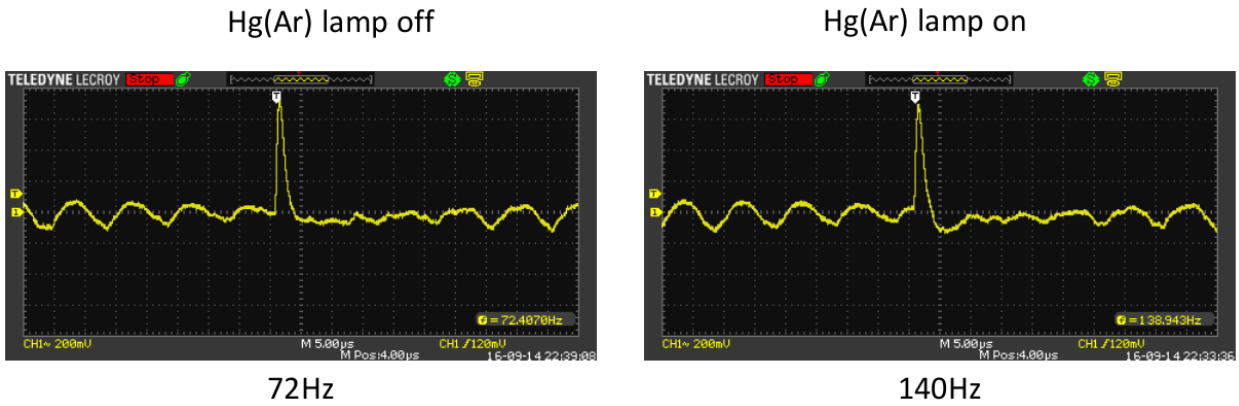

Figure 9 Oscilloscope pulses recorded for sealed tile #9 under ambient full atmosphere conditions, when exposed to a Hg(Ar) lamp. 1,000V was applied to each ALD-GCA-MCP corresponding to a gain of $3X10^6$. The pulse rate doubles when the lamp is turned on. The threshold trigger rate for the oscilloscope was set high due to periodic noise from the lamp.

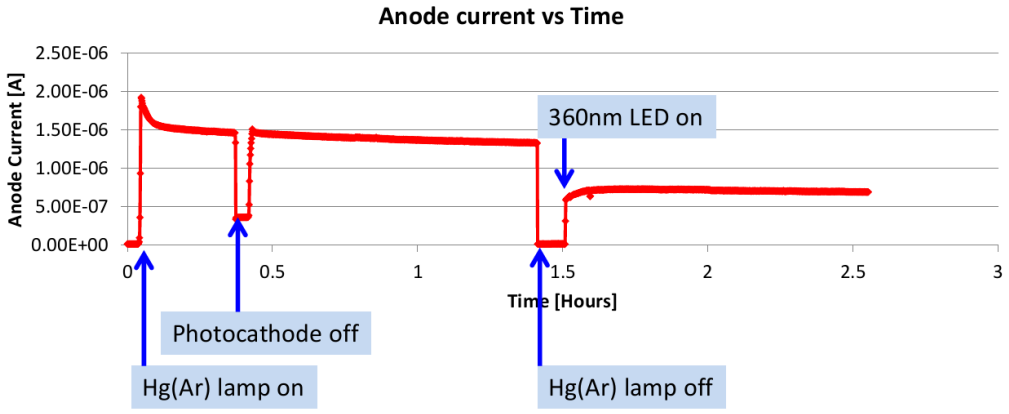

Figure 10, Ambient testing of Tile #9 under various illumination scenarios confirmed that the detector was operational.

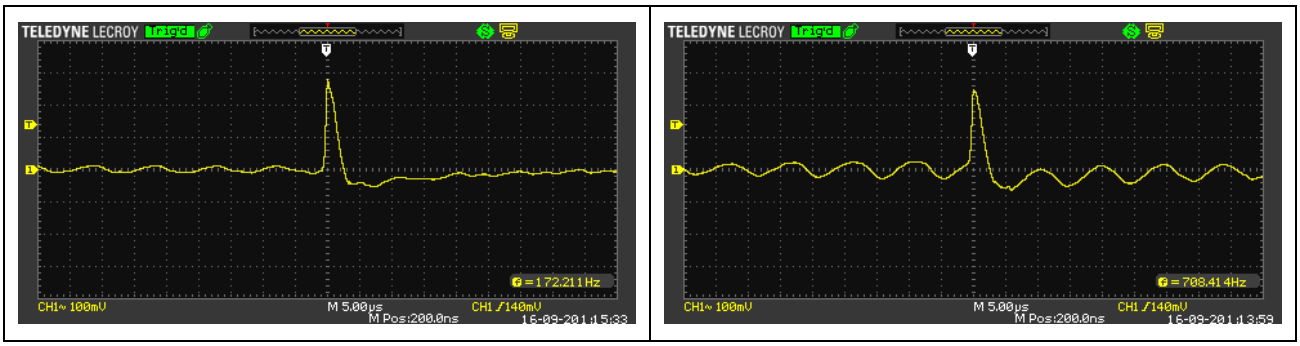

Figure 11 - Hg(Ar) Lamp-off (left), lamp-on (right) testing was repeated six days later under ambient pressure conditions with the output waveforms averaged over 32 pulses. 1,100 volts was applied to each of the MCPs, corresponding to a gain of $2X10^7$.

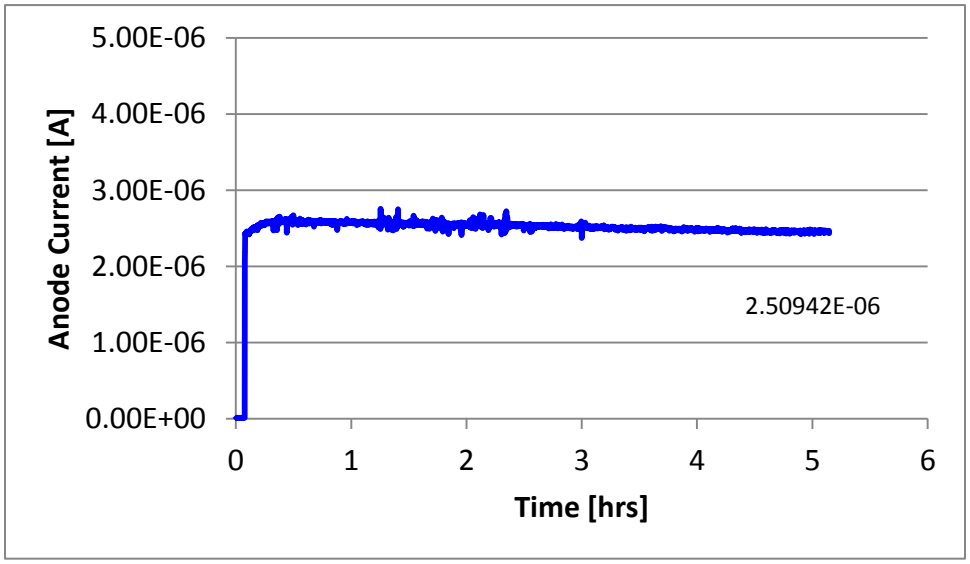

Figure 12 – Anode current vs. time measurement was repeated for LAPPD #9 on 9/20/2016 after 7 days, with the LED off, the dark current (I_{DARK}) was ~20nA, increasing to 2.5 micro-amps when exposed to 360nm with LED on.

"Lamp-off, lamp-on" testing was repeated six days after the tile was sealed, under ambient pressure conditions with the output waveforms averaged over 32 pulses, as shown in Figure 11. 1,100 volts was applied to each of the MCPs, corresponding to a gain of $2X10^7$. In these trials pulse rate increased by more than a factor of 4X from 172Hz to 708Hz. Anode current vs. time measurement was repeated after 7 days, with the LED off, the dark current (I_{DARK}) was ~20nA, increasing to 2.5 micro-amps when exposed to 360nm with LED on, as shown in Figure 12.

Comprehensive testing of the tile continues, with plans to characterize timing and operational stability vs. time. Production of additional tiles remains on pace, which will utilize the more efficient Na_2KSb bi-alkali photocathode.

Advanced LAPPD Development - Continued development of LAPPD^{TM}s and ALD-GCA-MCPs is being supported by grants from DOE, NASA and the National Geospatial Intelligence Agency (NGA) targeting specific requirements for high energy physics (HEP), space applications, and reduced cost. Areas of research include the development of alternate glasses for reduced noise, large-area ALD-GCA-MCPs with smaller pores for improved timing resolution, curved ALD-GCA-MCPs for compact detector devices for terrestrial and space applications, ceramic body LAPPD^{TM}s for improved durability and expanded design options for LAPPD anodes, and the development of ALD coatings that reduce thermal coefficient of resistance (TCR).

Long Life ALD-GCA-MCPs - Alkali elements (e.g. potassium and sodium) present in conventional lead silicate MCPs diffuse under high extracted charge affecting the gain performance of the MCP[18]. Potassium (^{40}K) contributes to dark current in conventional MCPs. The ALD-GCA-MCP fabrication process allows independent selection of the glass

substrate. Incom uses two proprietary glass formulations, referred to as C5 and C14. Incom's C5 glass is a Pyrex® like borosilicate material with reduced alkali content compared to conventional MCPs. It has less potassium content than conventional MCPs, which is why the dark current in Incom MCPs is substantially lower than in conventional MCPs[19,20]. Incom's C14 glass has virtually no alkali elements except as impurities. Dark count for Incom ALD-GCA-MCPs is 10-25 X lower compared to conventional MCPS (0.025-0.040 vs. 0.25-1.0), since they contain little or no radioactive isotopes, resulting in further enhanced signal to noise (S/N).

GEN II Ceramic Package – In a joint collaboration with the University of Chicago, Incom Inc. is developing a second generation LAPPD^{TM} with a ceramic package and options for either a borofloat or a fused silica top window. The ceramic package offers a number of advantages including higher strength, higher fracture toughness, and the ability to form near-net-shape components, by pressing the ceramic material while still in the green state. The ceramic also has a lower TanΔ, making it uniquely suited for a novel signal collection strategy referred to as "inside out". With "inside-out", amplified MCP signals impinge on a metallic ground plane coating the inside surface of the ceramic LTA, and capacitively couple through the ceramic base of the detector, to anodes on the outside. Anode design, whether pixilated pads or strip-lines, can be customized to meet the needs of specific customers. The notion of producing a generic detector body that can be later modified to meet specific customer needs has significant cost reduction implications. As shown in Figure 13 , preliminary trials show[21,22,23] that when a thin metal layer anode serves as a DC ground on the inside of the detector, 88% of an MCP fast signal pulse was capacitive coupled through the ceramic, to strips or pads on the outside.

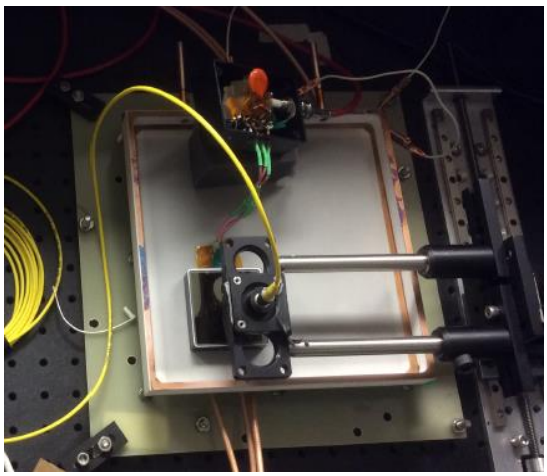

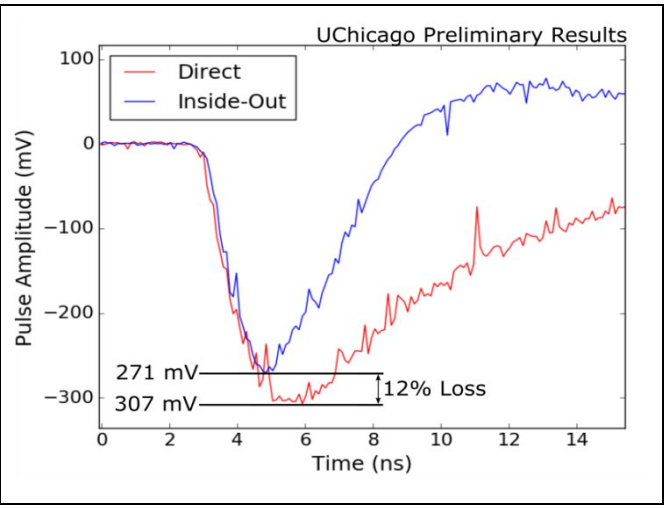

Figure 13 - A thin metal layer anode serves as a DC ground on the inside of the detector. 88% of an MCP fast signal pulse was capacitive coupled through the ceramic, to strips or pads on the outside.

Low TCR ALD-GCA-MCPs - All MCPs, including ALD-GCA-MCPs, exhibit semiconductor-like electrical behavior and are characterized by a negative TCR. When MCPs are cooled their resistance increases, and when they are heated, their resistance drops. For this reason, the resistance of all MCPs must be custom specified depending on the target operating temperature. This sensitivity to temperature changes presents a challenge for many terrestrial as well as space-based applications, including for detectors capable of operation either at room temperature or at cryogenic temperatures. Too low a resistance generates too much joule heat in the MCP and can lead to thermal runaway, while too high a resistance limits MCP recharge time and hence count rate capabilities[24]

A flatter relationship between temperature and resistance would make MCPs useful in environments with a wide range of temperatures, and would also improve count rate performance at any temperature. The ability to "tune" the TCR for conventional MCPs is severely limited since the resistive and emissive layers are formed together during a hydrogen reduction process applied to the underlying glass substrate. For the ALD-GCA-MCP process, selection of the substrate glass, and formation of the resistive and SEE layer are separate steps that can be independently tuned for optimal performance. Three variables, film thickness, ALD metal composition and content, and the ALD nanocomposite nanostructure hold promise for reducing the TCR of ALD coated MCPs:

Both resistance and TCR are known to be affected by film thickness. Jiang reported resistance and TCR for thin TaNx films deposited on polished Al2O3 ceramic substrates by reactive dc magnetron sputtering[25]. Their results show that the

TCR actually crosses over from negative to positive TCR at a layer thickness of about 50 nm. The authors attributed the electrical properties to the TaNx to the parallel connection of a surface layer with high resistivity and negative TCR and the underlying bulk layer with low resistivity and positive TCR. Understanding the thickness dependence for our Chem1 resistive material on the TCR will provide further control in achieving low-TCR MCPs.

Metal composition and content has been shown to affect the TCR of ALD-GCA-MCPs. Figure 14 is a plot of TCR vs. metal content for Chem1 and Chem2 coatings. The TCR slope ρ is different for the two materials, indicating that TCR is material dependent, and that with the right choice of material and composition can yield coatings with near-zero TCR that still exhibit reasonably high resistivity. Figure 14 also shows that Chem2 (Mo and Al2O3) has a lower TCR compared to Chem1 (W, and Al2O3).

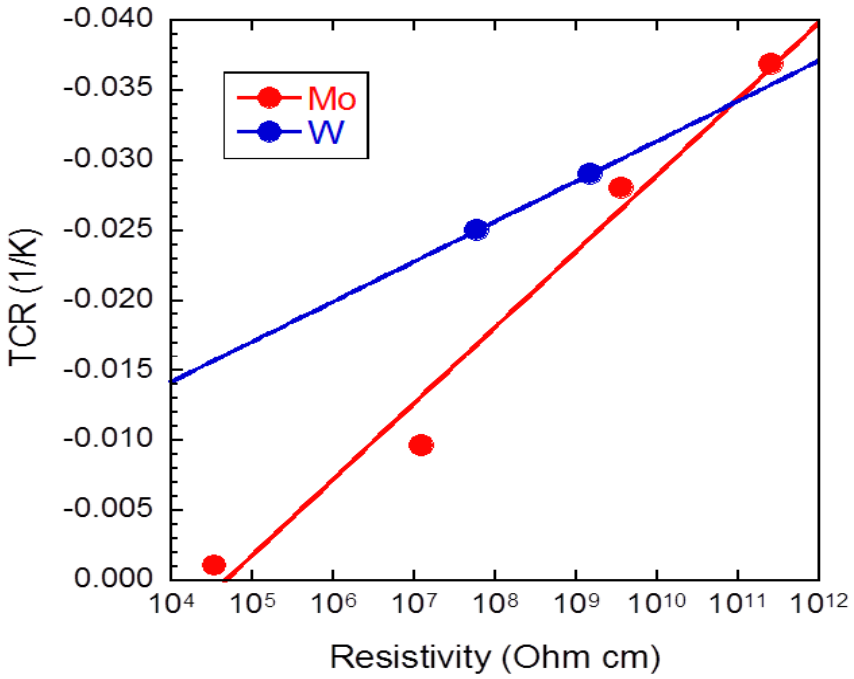

Figure 14 - Resistivity vs. TCR for Chem1 (W:Al_2O_3) and Chem2 (Mo:Al_2O_3) nanocomposite material. Data points represent different film compositions (decreased metal content with increased resistance), and demonstrate that the TCR is material dependent.

The nanocomposite structure of ALD-GCA-MCPs is can be readily varied depending on specific deposition process parameters. While an explicit relationship to TCR has not yet been demonstrated, this ability to control structure and performance provides encouragement for this development.

Conclusions and future plans - Progress on infrastructure and process development has been steady. In the 2½ years since beginning construction in April 2014, a pilot production infrastructure has been created, starting with nothing. An experienced team of scientists, engineers, and technicians was assembled enabling ALD-GCA-MCP and LAPPD™ process development commissioning trials to begin in December 2015.

No technical roadblocks or insurmountable barriers have been encountered since commissioning trials began in December 2015. Development trials progressed as follows: a) Routine operation of Incom integration & sealing tool operating at 10^{-10} Torr, b) demonstration of a repeatable 203mm X 203mm ALD-GCA-MCP fabrication process, c) multiple successful sidewall to top window sealing demonstrations, d) photocathode deposition trials, e) mock LAPPD™ assembly and sealing trials, followed by f) nine fully integrated LAPPD™ fabrication trials. A major program milestone was achieved with the production of a fully functional LAPPD #9 equipped with a 10nm thick Aluminum photocathode. The detector demonstrated a stable spark free operation at a gain of $2X10^7$ providing sensitivity to single photoelectrons in the UV spectral range. More detailed evaluation tests are on-going including measurements of time and spatial resolution, gain uniformity across the area and long term gain stability. A transition from "commissioning stage" to "exploitation" and routine pilot production is expected shortly after identified component and hardware improvements

are implemented and process experience is gained. Incom remains on-plan to deliver prototype "all glass" LAPPD^{TM}s to early adopters.

Acknowledgements - The authors wish to acknowledge the financial and advisory support provided by the DOE, NASA, and National Geospatial Intelligence Agency under the following contracts: DOE, DE-SC0009717, DOE DE-SC0011262 Phase II, DOE, DESC0015267, NASA, NNX15CG22P, NGA-IV, NGA-V, DOE DESC0015729, DOE DE-SC0009717 Phase IIA.

[1] Minot, M. J., et. al., "Pilot production & commercialization of LAPPD™"Nuclear Instruments and Methods in Physics Research A 787 (2015) 78–84

[2] A.U. Mane et el., "A novel atomic layer deposition method to fabricate economical and robust large area microchannel plates for photodetectors", Physics Procedia, 37, 722-732 (2012).

[3] J. W. Elam, A. U. Mane, J. A. Libera, J. N. Hryn, O. H. W. Siegmund, J. McPhate, M. J. Wetstein, A. Elagin, M. J. Minot, A. O'Mahony, R. G. Wagner, H. J. Frisch, W. M. Tong, A. D. Brodie, "Synthesis, Characterization, and Application of Tunable Resistance Coatings Prepared by Atomic Layer Deposition", ECS Trans. 2013 volume 58, issue 10, 249-261, DOI: 10.1149/05810.0249ecst

[4] A. U. Mane and J. W. Elam, "Atomic Layer Deposition of W:Al2O3 Nanocomposite Films with Tunable Resistivity",Chem. Vap. Deposition, 19, 186–193, (2013). doi: 10.1002/cvde.201307054

[5] A. O'Mahony et al., "Atomic layer deposition of alternative glass microchannel plates", J. Vac. Sci. Techn. A, 34, 01A128 (2016); doi: 10.1116/1.4936231

[6] Frisch, H.J., et al "RF strip-line anodes for Psec large-area MCP-based photodetectorsH Nuclear Instruments and Methods A71 (2013) 124.

[7] M. Wetstein, B.W. Adams , A. Elagin, H.J. Frisch, R. Obaid, E. Oberla , A. Vostrikov, R.G. Wagner, J. Wang, Timing characteristics of Large Area Picosecond Photodetectors Nuclear Instruments and Methods in Physics Research A 795 (2015) 1–11

[8] Henry J. Frisch, et. al., A Brief Technical History of the Large-Area Picosecond Photodetector (LAPPD) Collaboration, http://arxiv.org/abs/1603.01843 March 2016

[9] Report of the Particle Physics Project Prioritization Panel, http://lbne-old.fnal.gov/pdfs/Threefrontiers.pdf

[10] DOE, DE-SC0009717 "LAPPD Commercialization – Fully Integrated Sealed Detector Devices"

[11] Attribution for sketch: Ertley MCP Imaging Detectors for High Dynamic Range 2016_SORMA_

[12] Attribution for sketch: O.H.W. Siegmund

[13] O.H.W. Siegmund et al., NSS/MIC, IEEE.N45-1, pp.2063-2070 (2011)

[14] O.H.W. Siegmund, Advanced Maui Optical and Space Surveillance Technologies Conference (2012) .

[15] S.J. Jokela et al., Physics Procedia, 37, 740 – 747 (2012)

[16] Siegmund - LAPPD2 Hermetic Package Godparent Review, April 03, 2013

[17] A. Lyashenko, "Incom LAPPD", Presented at the Pico-Second Workshop, Kansas City, Sept 15-18 2016

[18] Then, A.M., and C.G. Pantano, "Formation and behavior of surface layers on electron emission glasses", Journal of Non-Crystalline Solids, 120, pp. 178-187, 1990.

[19] O.H.W. Siegmund, N. Richner, G. Gunjala, J.B. McPhate, A.S. Tremsin, H.J. Frisch, J. Elam, A. Mane, R. Wagner, C.A. Craven, M.J. Minot, "Performance Characteristics of Atomic Layer Functionalized Microchannel Plates" Proc. SPIE 8859-34, in press (2013).

[20] O.H.W. Siegmund, K. Fujiwara, R. Hemphill, S.R. Jelinsky, J.B. McPhate, A.S. Tremsin, J.V.Vallerga, H.J. Frisch, J. Elam, A. Mane, D.C. Bennis, C.A. Craven, M.A. Deterando, J.R.Escolas, M.J. Minot, and J.M. Renaud, "Advances in Microchannel Plates and Photocathodes for Ultraviolet Photon Counting Detectors," Proc. SPIE 8145, pp. 81450J-81450J-12 (2011).

[21] B.W. Adams,et al, "An internal ALD-based high voltage divider and signal circuit for MCP-based photodetectors", Nuclear Instruments and Methods in Physics Research A 780 (2015) 107–113

[22] Private Communication, Todd Seiss and Evan Angelico, University of Chicago. Inside-Out Tests of Incom Tiles, June 23, 2016

[23] Angelico, Evan et al., "Development of an affordable, sub-pico second photo-detector", University of Chicago, Poster 2016

[24] A.S. Tremsin et al., "Thermal dependence of electrical characteristics of micromachined silica microchannel plates", Rev. Sci. Instrum., 75(4), 1068-1072, (2004)

[25] H. Jiang et al., "Influences of film thickness on the electrical properties of TaN*x* thin films deposited by reactive DC magnetron sputtering" J. Mater. Sci. Technol., 26(7), 597, (2010)